AIP Applied Physics Letters

Electromagnon excitations in canted-spin multiferroics

Hong-Bo Chen and You-Quan Li

Citation: Appl. Phys. Lett. **102**, 252906 (2013); doi: 10.1063/1.4812346
View online: http://dx.doi.org/10.1063/1.4812346
View Table of Contents: http://apl.aip.org/resource/1/APPLAB/v102/i25
Published by the AIP Publishing LLC.

APPLIED PHYSICS LETTERS **102**, 252906 (2013)

Electromagnon excitations in canted-spin multiferroics

Hong-Bo Chen and You-Quan Li[a)]
Zhejiang Institute of Modern Physics and Department of Physics, Zhejiang University, Hangzhou 310027, People's Republic of China

(Received 14 April 2013; accepted 12 June 2013; published online 28 June 2013)

The dynamical interplay between magnetism and electric polarization in a multiferroic with a canted-spin order is investigated by extending the conventional spin-current mechanism. We unravel the magnetic and magnetoelectric excitations of the system and manifest the existence of two species of electromagnon excitations exhibiting unique selection rules. Our results suggest a route to accurately identify the underlying magnetoelectric coupling of a multiferroic via an optical probe, which is essential for controlling the electromagnons in future magnonic devices. *© 2013 AIP Publishing LLC*. [http://dx.doi.org/10.1063/1.4812346]

Magnetoelectric (ME) multiferroics is an intriguing class of materials that simultaneously possess ferroelectric and magnetic orders.[1] The recent resurgence of interest in these materials is largely inspired by the discovery of the giant ME effects enabling an efficient mutual control of the polarization and magnetization.[2] Multiferroic materials have led to great scientific interests in understanding the origin of the magnetically driven ferroelectricity. The known microscopic origins of ME coupling include spin-current,[3–5] exchange striction,[6] and *p*-*d* hybridization.[6,7] Furthermore, these rapidly emerging materials may also raise the appealing possibility of realizing innovative technological applications, such as, for example, a next generation of logic devices or information storage.[8–10]

In multiferroic systems, the cross-correlation between magnetic and ferroelectric orders can give rise to the appearance of an elementary excitation. The intrinsic low-energy excitations in multiferroics, termed electromagnon,[11] consist of hybridized magnon-phonon excitations which show strong electric–dipole active characteristic. Initially observed in $GdMnO_3$ and $TbMnO_3$,[11] the electromagnon has been detected in a variety of multiferroic materials. Especially, the behavior of electromagnon in non-collinear magnets shows complicated properties, i.e., there are two or more absorption peaks and unique selection rules.[12] Several models have also been proposed to account for the mechanisms of electromagnons, such as spin-current,[13–15] magnetic striction,[16] and *p*-*d* hybridization.[17] An even more fascinating aspect of this concept is the promising route to control the spin waves using the electric fields instead of magnetic fields. Recent observations of electrical control of magnons in multiferroic $BiFeO_3$ at room temperature reveal a possibility of implementing such a function.[18–22] A potential design of ultrasmall logic devices utilizing electromagnon excitations was also proposed.[23]

Despite several experimental and theoretical advances, our knowledge about electromagnon which is crucial for functionality remains very limited and further efforts are required. According to the conventional spin-current mechanism built on the inverse Dzyaloshinskii-Moriya (DM) interaction,[3] the ferroelectric polarization induced by the ordered non-collinear canted-spin structure is given by $\boldsymbol{p}_1 \propto \boldsymbol{e}_{ij} \times (\boldsymbol{S}_i \times \boldsymbol{S}_j)$, where $\boldsymbol{e}_{ij}$ is a unit vector connecting the two neighboring spins, $\boldsymbol{S}_i$ and $\boldsymbol{S}_j$. This idea has been of crucial importance in the recent discovery of various multiferroic materials.[1] More recently, Kaplan and Mahanti[24] further argued from the view point of symmetry that the DM interaction can also yield an additional contribution, i.e., $\boldsymbol{p}_2 \propto \boldsymbol{S}_i \times \boldsymbol{S}_j$ in canted-spin system. Note that such a *canted-spin-induced polarization* or *extended spin-current model* was recently claimed to take place in delafossite multiferroic $AgFeO_2$.[25] This model is particularly appealing as it may also be applicable to the other multiferroic materials whose ferroelectricity cannot be explained by the conventional spin-current model, such as delafossite compounds Cu XO_2 ($X =$ Fe, Cr),[26,27] $RbFe(MoO_4)_2$,[28] and $Cu_3Nb_2O_8$.[29] However, the practical consequences of the introduction of the additional $\vec{p}_2$ contribution on the dynamical ME effect have not been investigated so far in any detail and this is the problem we solve in this letter. The studies of electromagnon excitations provide a fertile ground not only to help unravel the underlying microscopic ME coupling in realistic materials but also to advance the practical applications of electromagnon in magnonics.

Our calculation is based on an extended spin-current mechanism for the underlying coupled ferroelectric and magnetic orders.[24] We consider an insulating multiferroic magnet as a frustrated one-dimensional spin chain along the *z*-axis with atomic displacement. According to Ref. 13, the full model Hamiltonian is then given by

$$H = H_S + H_{me} + H_{ph}, \qquad (1)$$

where the three parts are defined by

$$H_S = -\sum_{i,j} J(\boldsymbol{r}_i - \boldsymbol{r}_j)\boldsymbol{S}_i \cdot \boldsymbol{S}_j + \sum_i D(S_i^y)^2,$$

$$H_{me} = -\sum_i \boldsymbol{u}_i \cdot [\lambda_1 \boldsymbol{e}_z \times (\boldsymbol{S}_i \times \boldsymbol{S}_{i+1}) + \lambda_2 \boldsymbol{S}_i \times \boldsymbol{S}_{i+1}],$$

$$H_{ph} = \sum_i \left(\frac{\kappa}{2}\boldsymbol{u}_i^2 + \frac{1}{2M}\boldsymbol{p}_i^2\right).$$

a)Electronic mail: yqli@zju.edu.cn.

Here, the first term H_S describes the spin frustration arising from the competition exchange interactions, where $J(\boldsymbol{r}_i-\boldsymbol{r}_j)$ is the isotropic exchange coupling between $\boldsymbol{S}_i$ and $\boldsymbol{S}_j$ at positions $\boldsymbol{r}_i$ and $\boldsymbol{r}_j$. $D>0$ is the single-ion easy-plane (zx-plane) anisotropy. The term $H_{\rm me}$ denotes the spin-lattice coupling and its strength is denoted by λ_1 and λ_2, where $\boldsymbol{u}_i$ is the effective atomic displacement of the ion at ith unit cell. The displacement $\boldsymbol{u}_i$ is related to a local dipole by $\boldsymbol{p}_i=e^*\boldsymbol{u}_i$ with e^* the Born charge. The last term $H_{\rm ph}$ refers to the dynamics of the lattice field, where $\boldsymbol{p}_i$ is the canonically conjugate momentum of $\boldsymbol{u}_i$. M and κ in $H_{\rm ph}$ are the effective mass and stiffness coefficients of $\boldsymbol{u}_i$, respectively. Minimization of the Hamiltonian in Eq. (1) with respect to $\boldsymbol{u}_i$ yields

$$\boldsymbol{u}_i=\frac{\lambda_1}{\kappa}\boldsymbol{e}_z\times(\boldsymbol{S}_i\times\boldsymbol{S}_{i+1})+\frac{\lambda_2}{\kappa}\boldsymbol{S}_i\times\boldsymbol{S}_{i+1}. \tag{2}$$

For zx-plane spiral spins along the chain with the spin ground state $\boldsymbol{S}_i=S(\sin\phi_i,0,\cos\phi_i)$, Eq. (2) results in a uniform atomic displacement per unit cell along not only the x-axis but also the y-axis, i.e., $\boldsymbol{u}_i^0=(u_0^x,u_0^y,0)$ with $u_0^x=-\lambda_1S^2\sin(Qa)/\kappa$ and $u_0^y=\lambda_2S^2\sin(Qa)/\kappa$. Here, the angles $\phi_i=\boldsymbol{Q}\cdot\boldsymbol{r}_i$ define the relative orientation of the spins for a given ordering wave vector $\boldsymbol{Q}$, S is the magnitude of spin and a is the lattice constant. The resulting macroscopic electric polarization $\boldsymbol{P}=e^*\boldsymbol{u}_i^0$ will appear in the plane perpendicular to the chain direction (i.e., z-axis).

Regarding the dynamics of the system, we are interested in the low-energy excitations. We explore first the pure spin excitation corresponding to the magnetic part and treat the atomic displacement statically (i.e., $\boldsymbol{u}_i^0$) at this stage. For spiral spin order, it is convenient to introduce a rotating local coordinate system (ξ_i,η_i,ζ_i) for each spin.[30] The local ζ-axis is aligned to the classical spin direction at each site. For the zx-plane spiral spin, the transformation of spin components reads $\boldsymbol{S}_i=\tilde{\boldsymbol{S}}_iR_y^T(\phi_i)$ where $\boldsymbol{S}_i=(S_i^x,S_i^y,S_i^z)$, $\tilde{\boldsymbol{S}}_i=(S_i^\xi,S_i^\eta,S_i^\zeta)$, and $R_y^T(\phi_i)$ is the transpose of the three-dimensional rotation matrix about y-axis with rotation angle ϕ_i. We then can express the model Hamiltonian (1) in terms of the rotating local coordinates. Applying a Holstein-Primakoff (HP) transformation, the spin operators in the local reference frame become $S_i^+=\sqrt{2S}a_i$, $S_i^-=\sqrt{2S}a_i^\dagger$ and $S_i^\zeta=S-a_i^\dagger a_i$, where a_i and $a_i^\dagger$ are the magnon annihilation and creation operators, respectively. The linear spin wave Hamiltonian in the q space is given by

$$\begin{aligned}H=&H^{(0)}+\frac{1}{4}\sum_q(A_q+B_q)(a_q^\dagger a_q+a_qa_q^\dagger)\\&+(A_q-B_q)(a_qa_{-q}+a_q^\dagger a_{-q}^\dagger),\end{aligned} \tag{3}$$

where $H^{(0)}=-NJ_QS(S+1)-Nu_0S\sin(Qa)(S/2+1)$ is the classical energy of the system, N is the total number of spin sites, and J_q is the Fourier transform of $J(r_i)$ with the wavevector q given by $J_q=\sum_iJ(r_i)\exp(iqr_i)$. The coefficients A_q and B_q read

$$\begin{aligned}A_q&=2S[J_A+u_0(1-\cos(qa))\sin(Qa)],\\B_q&=2S[J_B+u_0\sin(Qa)],\end{aligned} \tag{4}$$

where $J_A=J_Q-(J_{q+Q}+J_{q-Q})/2$, $J_B=J_Q-J_q+D$ and $u_0=\lambda_2u_0^y-\lambda_1u_0^x$. The quadratic part of the Hamiltonian in Eq. (3) can be diagonalized with the help of Bogoliubov transformation, $a_q=\cosh\theta_qb_q+\sinh\theta_qb_{-q}^\dagger, a_{-q}^\dagger=\cosh\theta_qb_{-q}^\dagger+\sinh\theta_qb_q$, where $\tanh2\theta_q=-(A_q-B_q)/(A_q+B_q)$. We obtain

$$H=\sum_q\hbar\omega_q(b_q^\dagger b_q+1/2)+\text{const.}, \tag{5}$$

where the spin wave frequencies are

$$\omega_q=\sqrt{A_qB_q}. \tag{6}$$

Note that spin wave excitation mode ω_q is an even function of q and, at $q=0$, it is gapless Goldstone mode corresponding to the global rotation of spins around y axis. The spin-lattice coupling introduces an effective spin anisotropy[13,14] and yields an energy gap of the spin wave frequency at ordering wavevector Q. One can see in the following discussion that the spin fluctuations at $q=\pm Q$ is important for the association with the magnetoelectric excitation (i.e., electromagnon).

We now turn our attention to the dynamical interplay between the spins and the polarizations. At the lowest temperature region of the spiral ordered phase, S_i^ζ can be regarded as a constant and its fluctuation can be neglected. Thus for spin degrees of freedom, we only invoke S_i^ξ and S_i^η as dynamical parts. From term $H_{\rm me}$ in Eq. (1), one can find that phonon modes $\delta u_i^x,\delta u_i^y$ and δu_i^z are all coupled to spin order, which is in contrast to the case of the conventional spin-current model where only the transverse phonon mode δu_i^y couples to the spin order.[13] Therefore, S_i^ξ,S_i^η and δu_i^α $(\alpha=x,y,z)$ are taken as sufficiently small dynamical quantities to represent electromagnon at the leading order. To study these collective modes, we implement an equation of motion approach for the spin and displacement dynamics of the system. Thus, the magnetoelectric excitations are described by the Landau-Lifshitz equation

$$\dot{\boldsymbol{S}}_i=\boldsymbol{S}_i\times\boldsymbol{H}_i^{\rm eff}, \tag{7}$$

where $\boldsymbol{H}_i^{\rm eff}$ is the effective magnetic field. The equations of motion in real space for spin operators S_i^ξ and S_i^η are then of the form $\dot{S}_i^\xi=S_i^\eta H_i^\zeta-S_i^\zeta H_i^\eta, \dot{S}_i^\eta=S_i^\zeta H_i^\xi-S_i^\xi H_i^\zeta$, where $S_i^\zeta=S$ and the effective field $\boldsymbol{H}_i^{\rm eff}=(H_i^\xi,H_i^\eta,H_i^\zeta)$ in the rotating local frame is given by

$$\begin{aligned}H_i^\xi=&\sum_j2J(r_{ij})\cos(Qr_{ij})S_j^\xi+u_0\sin(Qa)(S_{i+1}^\xi+S_{i-1}^\xi)\\&+S\cos(Qa)[\lambda_1(\delta u_i^x-\delta u_{i-1}^x)-\lambda_2(\delta u_i^y-\delta u_{i-1}^y)],\\H_i^\eta=&\sum_j2J(r_{ij})S_j^\eta-2DS_i^\eta-(\lambda_2\tilde{u}_1^x+\lambda_1\tilde{u}_1^y+\lambda_2\tilde{u}_2^z),\\H_i^\zeta=&2S[J(Q)+u_0\sin(Qa)],\end{aligned}$$

where $r_{ij}=r_i-r_j, \tilde{u}_1^\alpha=S(\delta u_{i-1}^\alpha\cos\phi_{i-1}-\delta u_i^\alpha\cos\phi_{i+1})$ and $\tilde{u}_2^\alpha=S(\delta u_i^\alpha\sin\phi_{i+1}-\delta u_{i-1}^\alpha\sin\phi_{i-1})$. It should be noted that in arriving at these equations of motion, we have restricted to keep the first order of the small quantities (i.e.,

$S_i^{\xi,\eta}, \delta u_i^{x,y,z}$) and neglected their second and higher orders. Meanwhile, the equations of motion for $\delta \boldsymbol{u}_i$ and $\boldsymbol{p}_i$ are given as $\delta \dot{u}_i^\alpha = p_i^\alpha / M$ ($\alpha = x, y, z$) and

$$\dot{p}_i^x = -\kappa \delta u_i^x + \lambda_1 \tilde{S}^\xi + \lambda_2 \tilde{S}_1^\eta,$$
$$\dot{p}_i^y = -\kappa \delta u_i^y + \lambda_1 \tilde{S}_1^\eta - \lambda_2 \tilde{S}^\xi,$$
$$\dot{p}_i^z = -\kappa \delta u_i^z + \lambda_2 \tilde{S}_2^\eta,$$

where $\tilde{S}^\xi = S[-S\sin(Qa) + (S_i^\xi - S_{i+1}^\xi)\cos(Qa)]$, $\tilde{S}_1^\eta = S(S_i^\eta \cos\phi_{i+1} - S_{i+1}^\eta \cos\phi_i)$ and $\tilde{S}_2^\eta = S(S_{i+1}^\eta \sin\phi_i - S_i^\eta \sin\phi_{i+1})$. Then, the equations of motion in q-space read

$$\dot{S}_q^\xi = B_q S_q^\eta + S^2[\lambda_2 E_+^x(Q) + \lambda_1 E_+^y(Q) + i\lambda_2 E_-^z(Q)],$$
$$\dot{S}_q^\eta = -A_q S_q^\xi + S^2 \cos(Qa)(\lambda_1 \delta u_q^x - \lambda_2 \delta u_q^y)(1 - e^{-iqa}), \quad (8)$$

where $E_\pm^\alpha(X) = \delta u_{q-X}^\alpha (e^{-iqa} - e^{iXa})/2 \pm \delta u_{q+X}^\alpha (e^{-iqa} - e^{-iXa})/2$. On the other hand, $\delta \dot{u}_q^\alpha = \frac{1}{M} p_q^\alpha$ and

$$\dot{p}_q^x = -\kappa \delta u_q^x + \lambda_1 S F'(Q) + \lambda_2 S F_+(Q),$$
$$\dot{p}_q^y = -\kappa \delta u_q^y + \lambda_1 S F_+(Q) - \lambda_2 S F'(Q), \quad (9)$$
$$\dot{p}_q^z = -\kappa \delta u_q^z + i\lambda_2 S F_-(Q),$$

with $F'(X) = S_q^\xi (1 - e^{iqa})\cos(Xa) - S\sin(Xa)\delta_{q,0}$, $F_\pm(X) = S_{q-X}^\eta (e^{iXa} - e^{i(q-X)a})/2 \pm S_{q+X}^\eta (e^{-iXa} - e^{i(q+X)a})/2$. The coefficients A_q and B_q are given in Eqs. (4). Note that in the case of $\lambda_{1,2} = 0$, the spin waves are decoupled from phonon modes and we can derive the spin wave spectrum in Eq. (6) from Eqs. (8). When $\lambda_{1,2} \neq 0$, spin degrees of freedom and electrical polarization are coupled to each other. Especially, the transverse phonons δu_q^x and δu_q^y are coupled to S^ξ and S^η not only at $q \pm Q$ but also at q, while δu_q^z is also coupled to $S_{q\pm Q}^\eta$ due to λ_2. However, within the conventional spin-current model,[13] there is only coupling between transverse phonon mode δu_q^y and S^η which is just located at $q \pm Q$. Furthermore, it is worth noting that the uniform lattice deformations δu_0^x and δu_0^y are both coupled to $(S_Q^\eta - S_{-Q}^\eta)$, which describes the rotation of both the spin-spiral plane and the direction of the polarization along the z axis.[13,14] On the other hand, the longitudinal phonon mode δu_0^z is coupled to $(S_Q^\eta + S_{-Q}^\eta)$, which corresponds to the rotation of both the spin-spiral plane and the direction of the polarization along the x axis, while within the conventional spin-current model, the x-axis rotation of spin-spiral plane mode is not coupled directly to the polarization dynamics.[13]

Since the underlying electromagnons manifest themselves in the ac dielectric response of the system, we shall then identify the associated polarization fluctuations which are in connection with the optical experiments. The dielectric function $\varepsilon_{\alpha\alpha}(\omega)(\alpha = x, y, z)$ can be obtained from the Green's function through $\varepsilon_{\alpha\alpha}(\omega) = 1 - 4\pi(e^*)^2 G^R(u_q^\alpha u_{-q}^\alpha; \omega)$, where $G^R(AB;\omega)$ is the Fourier transformation of the retarded Green's function $G^R(AB; t - t')$ defined as $G^R(AB; t - t') = -i\theta(t - t')\langle [A(t), B(t')] \rangle$, with $A, B = u_q^\alpha, p_q^\alpha, S_q^\xi, S_q^\eta$ in our case. These Green's functions can be determined from a set of generic equations of motion whose Fourier transform satisfies $\omega \langle\langle A; B \rangle\rangle_\omega = \frac{1}{2\pi}\langle [A, B] \rangle + \langle\langle [A, H]; B \rangle\rangle_\omega$. Here, we denote $G^R(AB;\omega) = \langle\langle A; B \rangle\rangle_\omega$ and the frequencies of electromagnons are given by the poles of the Green's functions. In particular, as the optical experiments typically probe the modes near the zero wave vector, here we are interested in phonon modes near $q = 0$.[13] After some straightforward algebra, we can derive the polarization correlation functions

$$\langle\langle \delta u_0^\alpha; \delta u_0^\alpha \rangle\rangle = \frac{1}{2\pi M} \frac{1}{\omega^2 - \omega_0^2 + \dfrac{2\tilde{\lambda}_\alpha^2 S^3 \sin^2(Qa)\tilde{A}}{M(\omega^2 + \tilde{B}_\alpha)}}, \quad (10)$$

where $\alpha = x, y, z$, $\omega_0 = \sqrt{\kappa / M}$ is the frequency of the original phonon, $\tilde{\lambda}_x = \tilde{\lambda}_z = \lambda_2$, $\tilde{\lambda}_y = \lambda_1$, $\tilde{A} = -A_Q + a_{12}\omega_0^2/(\omega_0^2 - \omega^2)$,

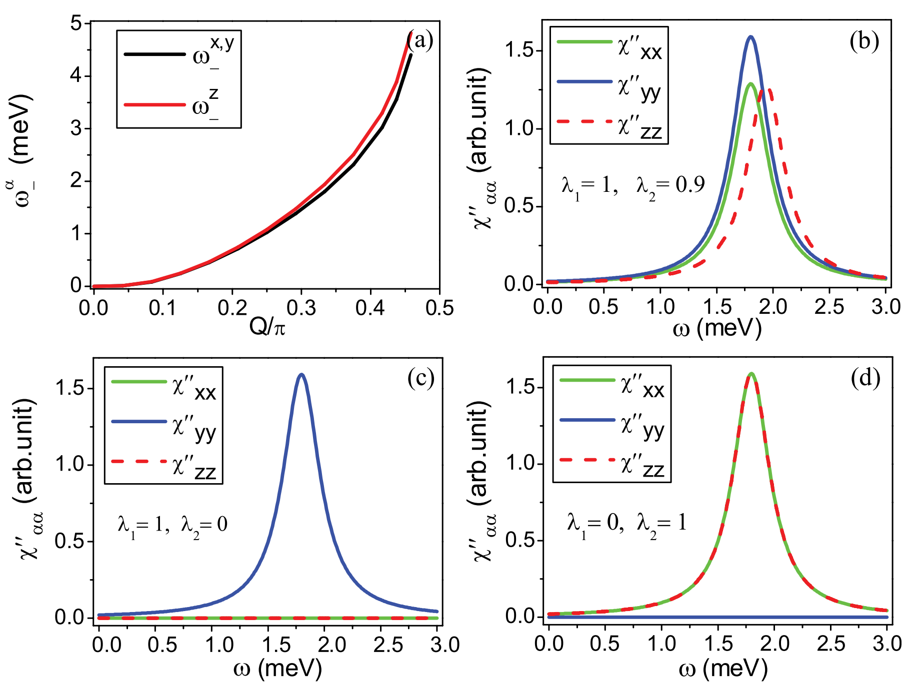

FIG. 1. (a) The electromagnons $\omega_-^\alpha (\alpha = x, y, z)$ as a function of the ordering wavevector Q. We assumed that the spiral spin order is realized by the competing exchange interactions and used the following values for the model:[4,13] nearest-neighbour exchange constant $J = 0.8$ meV, $D = 0.2$ meV, $S = 2$, $\lambda_{1,2} = 1$ meV/Å, and $\lambda/\kappa a = 10^{-2}$. (b)–(d) are the calculated electromagnon spectral shapes for $Qa = \pi/3$ with different polarizations and different values of the spin-lattice coupling constants.

$\tilde{B}_x = [B_Q - \frac{2\lambda_1^2 S^3}{\kappa}\sin^2(Qa)\omega_0^2/(\omega_0^2-\omega^2)]\tilde{A}$, $\tilde{B}_y = [B_Q - \frac{2\lambda_2^2 S^3}{\kappa}\sin^2(Qa)\omega_0^2/(\omega_0^2-\omega^2)]\tilde{A}$, $\tilde{B}_z = B_Q\tilde{A}$, and $a_{12} = 2(\lambda_1^2+\lambda_2^2)S^3\cos^2(Qa)(1-\cos(Qa))/\kappa$. In obtaining the above three phonon correlation functions via the Green function equation of motion, we have employed a decoupling approximation by neglecting the correlations such as $\langle\langle S^{\xi(\eta)}_{\pm 2Q}; u_0^\alpha\rangle\rangle$. From Eq. (10), we can easily see that the dielectric response would be expected to occur in all x, y, and z directions. On the other hand, in the absence of spin-lattice coupling λ_2, the low-frequency behavior exhibits only in the $\langle\langle\delta u_0^y;\delta u_0^y\rangle\rangle$, which is consistent with the conventional spin-current model.[13] The poles of the correlation functions correspond to the energies of the elementary excitations of the coupled system. As for realistic materials,[4,13] we can reasonably assume $D, J \ll \kappa a^2$ and $\lambda_{1,2} \ll \kappa a$. Each polarization correlation function possesses two poles $\omega_\pm$. One is $\omega_+^\alpha \approx \omega_0\,(\alpha = x,y,z)$, which are the original phonon modes contributing to the dielectric response. The other one is the low-energy hybridized collective mode, i.e., the electromagnon. We observe that the aforementioned z-axis rotation mode coupling to the polarization dynamics leads to nearly the same low-energy behavior of the polarization correlation function $\omega_-^x = \omega_-^y \approx (2SDA_Q - a_{12}B_Q)^{1/2}$. Especially, along the spin chain direction, there is also a low-energy mode around $\omega_-^z \approx (2SDA_Q - a_1A_Q - a_{12}B_Q)^{1/2}$, with $a_1 = -2\lambda_1^2 S^3\sin^2(Qa)/\kappa$, which corresponds to the aforementioned x-axis rotation mode coupling to the polarization dynamics. It is worth noting that such an additional electromagnon mode is absent from the conventional spin-current model.[13] Fig. 1(a) shows the three electromagnons ω_-^α as a function of the ordering wave vector Q. Let us further discuss the spectral shapes. The imaginary part of the *ac* susceptibility is $\chi''(AB;\omega) = -\mathrm{Im}G^R(AB;\omega)$. With the poles $\omega_\pm^\alpha$, one can write $G^R(u_0^\alpha u_0^\alpha;\omega) = \sum_\pm I_\pm^\alpha/(\omega^2 - (\omega_\pm^\alpha)^2)$ with the intensities $I_\pm^\alpha$ given by $I_-^\alpha = \tilde{a}_\alpha A_Q/2\pi M[(\omega_+^\alpha)^2 - (\omega_-^\alpha)^2]$ and $I_+^\alpha = [\tilde{b}_\alpha A_Q\omega_0^2/b_0 - (\omega_-^\alpha)^2]/2\pi M[(\omega_+^\alpha)^2 - (\omega_-^\alpha)^2]$, where $\tilde{a}_x = \tilde{a}_z = a_2 = 2\lambda_2^2 S^3\sin^2(Qa)/\kappa, \tilde{a}_y = -a_1, \tilde{b}_x = a_2, \tilde{b}_y = -a_1$, $\tilde{b}_z = a_2 - a_1$, and $b_0 = a_{12}B_Q + 2Su_0\sin(Qa)A_Q$. In the spectral shapes, these poles represent Delta functions at the pole positions. Calculated electromagnon (ω_-^α) spectral shapes for different polarizations and spin-lattice coupling constants are shown in Figs. 1(b)–1(d). The Delta functions are replaced by the Lorentzians with width $\epsilon = 0.2$. It is shown that the selection rules are closely related to the spin-lattice coupling constants. These special characteristics of electromagnon revealed by the extended spin-current model[24] can be verified by further optical experiments.

In conclusion, we have studied and identified the magnetic and electromagnon excitations of the non-collinear canted-spin order in a magnetically driven multiferroic. We predicted an additional electromagnon mode which corresponds to the rotation mode of the spin plane around the direction perpendicular to the axis of the helix. Thus, the presence or absence of this electromagnon mode in an optical probe may provide a convenient way to determine whether an extended spin-current model[24] is the underlying ME coupling mechanism for some particular multiferroics. The present observations may also offer an useful clue to control the electromagnons in future magnonic devices.

This work was supported by NSF-China (Grant Nos. 11074216 and 11274272) and the Fundamental Research Funds for the Central Universities in China.

[1] M. Fiebig, J. Phys. D: Appl. Phys. **38**, R123 (2005); W. Eerenstein, N. D. Mathur, and J. F. Scott, Nature **442**, 759 (2006); S.-W. Cheong and M. Mostovoy, Nature Mater. **6**, 13 (2007); K. F. Wang, J.-M. Liu, and Z. F. Ren, Adv. Phys. **58**, 321 (2009); G. Catalan and J. F. Scott, Adv. Mater. **21**, 2463 (2009).
[2] T. Kimura, T. Goto, H. Shintani, K. Ishizaka, T. Arima, and Y. Tokura, Nature **426**, 55 (2003); J. Wang, J. B. Neaton, H. Zheng, V. Nagarajan, S. B. Ogale, B. Liu, D. Viehland, V. Vaithyanathan, D. G. Schlom, U. V. Waghmare, N. A. Spaldin, K. M. Rabe, M. Wuttig, and R. Ramesh, Science **299**, 1719 (2003).
[3] H. Katsura, N. Nagaosa, and A. V. Balatsky, Phys. Rev. Lett. **95**, 057205 (2005).
[4] I. A. Sergienko and E. Dagotto, Phys. Rev. B **73**, 094434 (2006).
[5] M. Mostovoy, Phys. Rev. Lett. **96**, 067601 (2006).
[6] C. Jia, S. Onoda, N. Nagaosa, and J. H. Han, Phys. Rev. B **76**, 144424 (2007).
[7] T. Arima, J. Phys. Soc. Jpn. **76**, 073702 (2007).
[8] J. F. Scott, Nature Mater. **6**, 256 (2007).
[9] Y. Zhang, Z. Li, C. Deng, J. Ma, Y. Lin, and C.-W. Nan, Appl. Phys. Lett. **92**, 152510 (2008).
[10] C. Jia and J. Berakdar, Appl. Phys. Lett. **95**, 012105 (2009).
[11] A. Pimenov, A. A. Mukhin, V. Yu. Ivanov, V. D. Travkin, A. M. Balbashov, and A. Loidl, Nat. Phys. **2**, 97 (2006).
[12] A. M. Shuvaev, A. A. Mukhin, and A. Pimenov, J. Phys.: Condens. Matter **23**, 113201 (2011).
[13] H. Katsura, A. V. Balatsky, and N. Nagaosa, Phys. Rev. Lett. **98**, 027203 (2007).
[14] C. Jia and J. Berakdar, Eur. Phys. Lett. **85**, 57004 (2009).
[15] H. B. Chen, Y. Zhou, and Y.-Q. Li, J. Phys.: Condens. Matter **23**, 066002 (2011).
[16] M. P. V. Stenberg and R. de Sousa, Phys. Rev. B **80**, 094419 (2009); R. V. Aguilar, M. Mostovoy, A. B. Sushkov, C. L. Zhang, Y. J. Choi, S.-W. Cheong, and H. D. Drew, Phys. Rev. Lett. **102**, 047203 (2009); M. Mochizuki, N. Furukawa, and N. Nagaosa, *ibid.* **104**, 177206 (2010).
[17] S. Miyahara and N. Furukawa, J. Phys. Soc. Jpn. **80**, 073708 (2011).
[18] R. de Sousa and J. E. Moore, Phys. Rev. B **77**, 012406 (2008).
[19] R. de Sousa and J. E. Moore, Appl. Phys. Lett. **92**, 022514 (2008).
[20] A. Kumar, N. M. Murari, and R. S. Katiyar, Appl. Phys. Lett. **92**, 152907 (2008).
[21] P. Rovillain, R. de Sousa, Y. Gallais, A. Sacuto, M. A. Méasson, D. Colson, A. Forget, M. Bibes, A. Barthélémy, and M. Cazayous, Nature Mater. **9**, 975 (2010).
[22] A. Kumar, J. F. Scott, and R. S. Katiyar, Appl. Phys. Lett. **99**, 062504 (2011).
[23] M. P. Kostylev, A. A. Serga, T. Schneider, B. Leven, and B. Hillebrands, Appl. Phys. Lett. **87**, 153501 (2005); A. Khitun, D. E. Nikonov, and K. L. Wang, J. Appl. Phys. **106**, 123909 (2009).
[24] T. A. Kaplan and S. D. Mahanti, Phys. Rev. B **83**, 174432 (2011).
[25] N. Terada, D. D. Khalyavin, P. Manuel, Y. Tsujimoto, K. Knight, P. G. Radaelli, H. S. Suzuki, and H. Kitazawa, Phys. Rev. Lett. **109**, 097203 (2012).
[26] T. Nakajima, S. Mitsuda, S. Kanetsuki, K. Prokes, A. Podlesnyak, H. Kimura, and Y. Noda, J. Phys. Soc. Jpn. **76**, 043709 (2007).
[27] S. Seki, Y. Onose, and Y. Tokura, Phys. Rev. Lett. **101**, 067204 (2008).
[28] M. Kenzelmann, G. Lawes, A. B. Harris, G. Gasparovic, C. Broholm, A. P. Ramirez, G. A. Jorge, M. Jaime, S. Park, Q. Huang, A. Ya. Shapiro, and L. A. Demianets, Phys. Rev. Lett. **98**, 267205 (2007).
[29] R. D. Johnson, S. Nair, L. C. Chapon, A. Bombardi, C. Vecchini, D. Prabhakaran, A. T. Boothroyd, and P. G. Radaelli, Phys. Rev. Lett. **107**, 137205 (2011).
[30] T. Nagamiya, in *Solid State Physics*, edited by F. Seitz, D. Turnbull, and H. Ehrenreich (Academic Press, New York, 1967), Vol. 20, p. 305.